



Perspective—Electrochemical Stability of Water-in-Salt Electrolytes

Ruben-Simon Kühnel,^{1,*,z} David Reber,^{1,2,=} and Corsin Battaglia¹

¹Empa, Swiss Federal Laboratories for Materials Science and Technology, 8600 Dübendorf, Switzerland

²École Polytechnique Fédérale de Lausanne, Institut des Matériaux, 1015 Lausanne, Switzerland

The water-in-salt approach has expanded the electrochemical stability window of aqueous electrolytes, enabling novel aqueous batteries with relatively high cell voltages and energy densities. However, the stability of these electrolytes tends to be overestimated. The instability of the electrolyte is typically masked by high rates and a large excess amount of electrolyte present in lab cells. Based on a discussion of practical cells, we revisit voltammetry data and offer guidelines for a more stringent evaluation of electrochemical stability window data.

© 2020 The Author(s). Published on behalf of The Electrochemical Society by IOP Publishing Limited. This is an open access article distributed under the terms of the Creative Commons Attribution 4.0 License (CC BY, <http://creativecommons.org/licenses/by/4.0/>), which permits unrestricted reuse of the work in any medium, provided the original work is properly cited. [DOI: 10.1149/1945-7111/ab7c6f]



Manuscript submitted December 23, 2019; revised manuscript received February 15, 2020. Published March 23, 2020. *This paper is part of the JES Focus Issue on Challenges in Novel Electrolytes, Organic Materials, and Innovative Chemistries for Batteries in Honor of Michel Armand.*

Water has many excellent properties as electrolyte solvent. It possesses a high dielectric constant, low viscosity, and is non-toxic, non-flammable, and inexpensive. However, its major drawback is its limited electrochemical stability window (ESW) of thermodynamically only 1.23 V at 25 °C. This has generally limited the voltage of aqueous batteries to ≤ 1.5 V with the exception of the lead-acid battery reaching 2.1 V when fully charged. Through a combination of bulk, interface, and interphase effects, highly-concentrated aqueous solutions based on lithium perfluoroalkylsulfonamide and related salts have wider ESWs than traditional aqueous electrolytes used in e.g. nickel-metal hydride or lead-acid batteries.^{1–4} Molecular dynamics simulations indicate that particularly bis(trifluoromethanesulfonyl)imide (TFSI) anions accumulate at the electrode surface upon positive polarization, establishing a water-depletion zone that leads to higher oxidative stability of such electrolytes.² The increased reductive stability has been linked to the formation of a solid-electrolyte interphase on the anode side from decomposition of the lithium salt.^{1,3} In analogy to the solvent-in-salt approach,⁵ these electrolytes are also called water-in-salt electrolytes as they contain more salt than water by weight and volume.¹

The relatively wide ESW of water-in-salt electrolytes has enabled the development of novel, mostly intercalation-type, aqueous batteries with higher cell voltages than previously possible, narrowing the gap in voltage compared to cells based on organic electrolytes.^{1,6–9}

Current Status

The ESW of water-in-salt electrolytes such as 21 mol kg⁻¹ (21 m) LiTFSI has been reported to be as high as 3 V.^{1,7,10} This has enabled stable cycling of high-voltage cathode materials such as LiMn₂O₄ and Na₃(VOPO₄)₂F over several hundred cycles even at low charge/discharge rates.^{1,9,11} In combination with anode protection strategies, e.g. carbon coatings or hydrophobic polymer coatings, stable cycling was also demonstrated with TiO₂, Li₄Ti₅O₁₂, NaTi₂(PO₄)₃, and even graphite anodes.^{6,8,9,12}

However, an increasing number of studies is proposing batteries and supercapacitors with increasingly higher cell voltages. In some cases, the cell voltage is obviously too high as in the case of >3 V supercapacitors.^{13,14} In other cases, stable cycling was achieved at high rates, but the low rate performance is not reported or relatively fast capacity fading is observed.^{7,10}

These high-voltage devices usually have in common a low active material mass loading (≤ 5 mg cm⁻²) and a large amount of electrolyte (typically ~ 100 μ l cm⁻² with respect to the electrode area). Together with the often-employed high rates of ≥ 5 C, the stability of the electrolyte under more practical conditions is difficult to assess. When a cell is operated at high rates, the electrolyte is subjected to strongly reducing or oxidizing conditions for a much shorter time per cycle than at low rates. Hence, the current rate has a significant impact on the decomposition rate of the electrolyte per cycle. Realistic cells with high mass loadings (≥ 20 mg cm⁻²) would potentially not be able to support such high rates due to transport limitations in the electrolyte. Finally, the onset of detrimental effects from water hydrolysis, e.g. salt precipitation or (local) pH change,^{15,16} can be delayed for a long time when using large amounts of electrolyte as the relative change in electrolyte composition is then small.

Future Needs

How much electrolyte would a realistic battery based on water-in-salt electrolytes contain? Considering that the lithium-ion conductivity of typical water-in-salt electrolytes at room temperature is on the order of 1–7 mS cm⁻¹,^{7,17} i.e. comparable to that of carbonate-based organic electrolytes,¹⁸ the distance between current collectors composed of the thickness of anode, separator, and cathode should be similar to that in commercial lithium-ion batteries. Figure 1a shows the evolution of the overpotential stemming from the electrolyte resistance with increasing distance between current collectors for three hypothetical cells. The assumptions here are a lithium-ion conductivity of 3 mS cm⁻¹ at room temperature and of 0.1 mS cm⁻¹ for the low temperature scenario. For the high-energy and high-power batteries, we consider areal capacities and current rates of 5 and 2 mAh cm⁻² and C/5 and 10 C, respectively.

For these three scenarios, Ohmic losses are negligible up to the considered maximum distance between current collectors (neglecting electrode tortuosity) of 1 mm for the high-energy battery operated at room temperature. For the other two scenarios, Ohmic losses stemming from the electrolyte already exceed 100 mV for a distance of 100 and 150 μ m, respectively. Such an overpotential results in a loss in energy efficiency of 9.5% for a hypothetical cell with an average voltage of 2.0 V (see Fig. 1b).¹⁹ Hence, the electrode distance of practical cells based on water-in-salt electrolytes should be limited to enable high energy efficiency. This is in contrast to lead-acid batteries, whose sulfuric acid electrolyte has a room temperature conductivity that is three orders of magnitudes higher,²⁰ enabling larger electrode distance and thickness. Another argument for limiting the electrode distance in water-in-salt

*These authors contributed equally to this work.

^zE-mail: ruben-simon.kuehnel@empa.ch

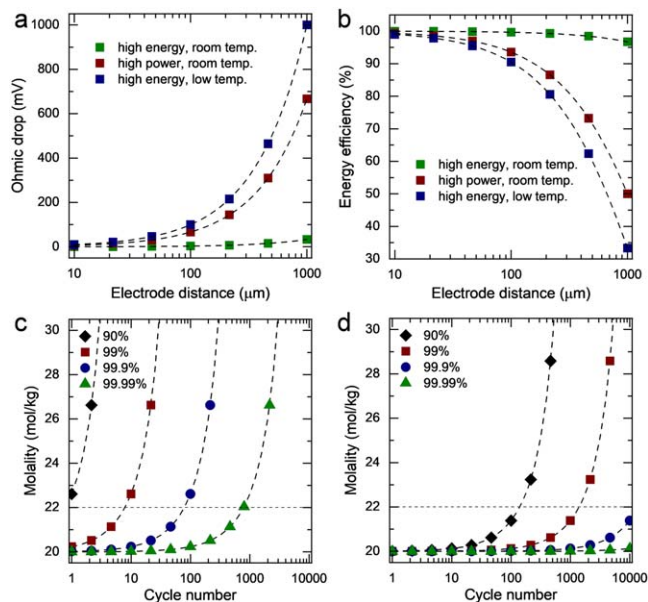


Figure 1. (a) Calculated dependence of the overpotential stemming from the bulk resistance of the electrolyte (Ohmic drop) on the electrode distance for three hypothetical cell scenarios. The assumptions are a conductivity of 3 mS cm^{-1} at room temperature (room temp.) and of 0.1 mS cm^{-1} at low temperature (low temp.). For the high-energy and high-power cells, areal capacities and current rates of 5 and 2 mAh cm^{-2} and $C/5$ and 10 C were considered, respectively. (b) The resulting effect of the Ohmic drop on the energy efficiency of a hypothetical 2.0 V cell. (c), (d) Calculated change of the electrolyte concentration with cycle number for (c) a realistic cell and (d) a typical lab cell. The calculation was carried out for Coulombic efficiencies of 90% , 99% , 99.9% , and 99.99% . For the realistic cell and lab cell, areal capacities of 5 and 0.5 mAh cm^{-2} were considered, respectively. The only other difference between the two cells is the amount of electrolyte: $5.6 \mu\text{l cm}^{-2}$ for the realistic cell (based on $2 \times 100 \mu\text{m}$ thick electrodes with a porosity of 25% and a $15 \mu\text{m}$ thick separator with a porosity of 40%) and $100 \mu\text{l cm}^{-2}$ for the lab cell. 20 m LiTFSI was chosen as (initial) electrolyte. The dashed horizontal line in (c) and (d) marks the onset concentration for crystallization of 22 mol kg^{-1} considered for the discussion.

electrolyte-based cells, and hence the amount of electrolyte, is the high cost of most water-in-salt electrolytes that stems from the high price and concentration of the employed salts.

As water-in-salt electrolytes are typically operated near the solubility limit of the salt or salt combination, water loss can lead to salt crystallization in the cell.⁹ Crystallization can lead to pore clogging, capacity loss, and an increase in cell resistance.^{9,15} Figures 1c and 1d compares the change in electrolyte concentration with cycle number for a realistic high-energy cell as established above and a typical lab cell under the assumption that the irreversible capacity is solely due to water hydrolysis.

For the realistic cell, we assume an areal capacity of 5 mAh cm^{-2} and for the lab cell 0.5 mAh cm^{-2} . The only other difference between the two cells is the amount of electrolyte: $5.6 \mu\text{l cm}^{-2}$ for the realistic cell (derived from $2 \times 100 \mu\text{m}$ thick electrodes with a porosity of 25% and a $15 \mu\text{m}$ thick separator with a porosity of 40%) and $100 \mu\text{l cm}^{-2}$ for the lab cell. The value of $5.6 \mu\text{l cm}^{-2}$ for a cell with a capacity of 5 mAh cm^{-2} corresponds well to the range of 1.3 to 1.5 grams of electrolyte per Ampere hour of cell capacity reported in literature for commercial lithium-ion batteries, considering the higher density of water-in-salt electrolytes (our assumption in this study: 1.75 g cm^{-3}) compared to that of commercial liquid organic electrolytes ($\sim 1.3 \text{ g cm}^{-3}$): $5.6 \mu\text{l cm}^{-2} \times 1.75 \text{ g cm}^{-3} / 5 \text{ mAh cm}^{-2} = 1.96 \text{ g Ah}^{-1}$.^{21,22} In the example, we consider a 20 m LiTFSI solution as (initial) electrolyte. If the Coulombic efficiency is only $\sim 90\%$, as is sometimes the case for slowly-cycled water-in-salt electrolyte-based cells reported in literature,^{7,10} the electrolyte

concentration of a realistic cell rapidly increases and exceeds the assumed solubility limit of 22 m after less than one cycle. Only cells displaying a Coulombic efficiency of $\geq 99.99\%$ can be cycled for more than 500 cycles. In contrast, the lab cell can be cycled for more than 100 cycles even if the Coulombic efficiency is as low as 90% . Hence, excess electrolyte clearly acts as cycle-life booster. This calculation ignores other detrimental effects of water hydrolysis such as local pH changes that can lead to active material degradation and current collector corrosion.^{16,23}

While the present study focuses on the electrochemical stability of the electrolyte and its effect on cycle life and energy efficiency, a comprehensive evaluation of new cell components in terms of all relevant performance metrics is desirable to assess their practical relevance.^{24,25} For example, the gravimetric energy density of batteries based on highly-concentrated electrolytes is slightly lower, all else being equal, due to the higher density of such electrolytes compared to traditional more dilute electrolytes (e.g., 1 M LiPF_6 in ethylene carbonate:dimethyl carbonate $1:1$ (by weight) has a density of 1.30 g cm^{-3} at 24°C , whereas $27.8 \text{ m Li(TFSI)}_{0.7}(\text{LiBETI})_{0.3}$ has a density of 1.78 g cm^{-3} at 25°C).^{7,22}

Considering that practical cells based on water-in-salt electrolytes require Coulombic efficiencies of $\geq 99.9\%$ at low rates to enable sufficient cycle life, rather strict criteria have to be used when determining the ESW of water-in-salt electrolytes to avoid a mismatch between reported ESW and cycling stability under realistic conditions. For this purpose, we revisited electrochemical stability data for the archetypical $\text{H}_2\text{O-LiTFSI}$ system. The ESW of electrolytes is most commonly determined via voltammetry experiments using (inert) metal working electrodes.¹⁸ A common criterion for the determination of the ESW from voltammetry data is a cut-off current density.²⁶ However, most water-in-salt electrolyte studies state a (wide) ESW without mentioning the criterion used to analyze the voltammetry data that the reported ESW is based on.

To study the effect of cut-off current density on the apparent ESW, we recorded voltammograms of aqueous LiTFSI solutions at a scan rate of 0.1 mV s^{-1} using stainless steel and gold working electrodes for the reductive and oxidative stability, respectively (Fig. 2a). All measurements were carried out in three-electrode Swagelok cells with a Bio-Logic VMP3 electrochemical workstation. Activated carbon-based pellets were used as counter electrode, a miniature Ag/AgCl electrode (eDAQ) was used as reference electrode, and a Whatman type GF/D glass microfiber filter drenched with $150 \mu\text{l}$ of electrolyte was used as separator. 12 mm disks of stainless steel (grade 1.4310, Brütsch/Rüegger Werkzeuge AG) or a 1 mm gold disk electrode from eDAQ were used as reference electrode, respectively.

We then determined the cathodic and anodic stability limits for different LiTFSI concentrations using different cut-off current densities (see Fig. 2b). For a cut-off current density of $50 \mu\text{A cm}^{-2}$, which corresponds to the nearly vertical parts of the current density–potential curves, we obtain an unrealistically wide ESW of 2.6 V already for the lowest concentration of 1 m . Hence, this criterion is clearly too loose. A much smaller cut-off current density of $2 \mu\text{A cm}^{-2}$ results in more realistic ESWs of 1.4 – 1.5 V for the 1 m , 7 m , and 14 m LiTFSI concentrations. For the 21 m LiTFSI solution, we obtain an ESW of 2.1 V , while for the $27.8 \text{ m Li(TFSI)}_{0.7}(\text{LiBETI})_{0.3}$ (LiBETI = lithium bis(pentafluoroethanesulfonyl)imide) solution an ESW of 2.4 V is obtained.⁷

Figure 2c shows the evolution of the apparent ESW of 21 m LiTFSI with increasing cut-off current density. Using a threshold of $100 \mu\text{A cm}^{-2}$, our results confirm the reported ESW of 3 V . When lowering the cut-off from 100 to $5 \mu\text{A cm}^{-2}$, the ESW slowly decreases from 3.1 to 2.7 V , while it drops to 2.1 V for a limit of $2 \mu\text{A cm}^{-2}$. Tying this current density back to a Coulombic efficiency target of e.g. 99.9% is not straightforward as the measured current density of such a voltammetry experiment depends on the scan rate, type of working electrode, and to a certain extent the geometry of the employed cell. For a cell with an areal capacity of 5 mAh cm^{-2} operated at a current rate of $C/5$, a Coulombic efficiency

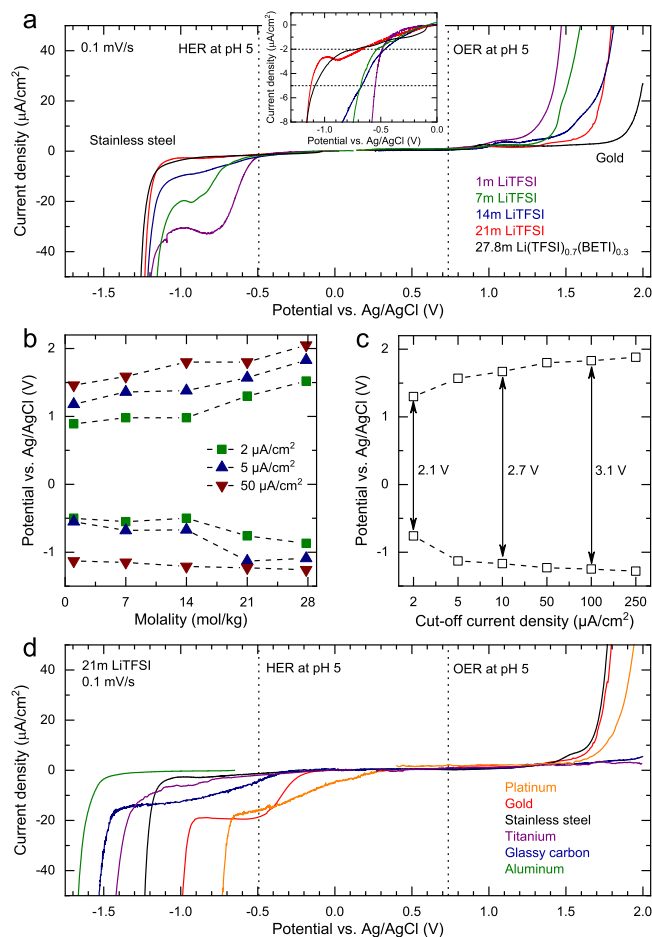


Figure 2. Electrochemical stability windows of degassed aqueous LiTFSI solutions of various concentrations. (a) Linear sweep voltammograms on stainless steel (for the reductive stability) and gold (for the oxidative stability), respectively. The thermodynamic onsets of the hydrogen and oxygen evolution reactions for a pH of 5 are shown as dashed vertical lines. The inset is a magnification of the low-current region of the cathodic scan. (b) Stability limits of the electrolytes as determined by applying three different threshold current densities to the voltammetry data shown in (a). (c) Stability window of 21 m LiTFSI as a function of cut-off current density. (d) Linear sweep voltammograms for 21 m LiTFSI on platinum, gold, stainless steel (SS), titanium, glassy carbon (GC), and aluminum. The pH of all solutions was adjusted to a value of ~ 5 . All experiments were carried out at room temperature at a scan rate of 0.1 mV s^{-1} .

of 99.9% corresponds to an average irreversible current density of $1 \mu\text{A cm}^{-2}$. As many applications involve keeping the battery at a state-of-charge of at least 50% and as even a Coulombic efficiency of 99.9% does not enable hundreds of cycles, a lower current density for water decomposition of $<1 \mu\text{A cm}^{-2}$ appears desirable, if refilling is no option. Nevertheless, the water-in-salt approach clearly improves the electrochemical stability of aqueous electrolytes. In particular, the oxidative stability of neutral-pH water-in-salt electrolytes appears to be (at least) on par with that of conventional carbonate-based electrolytes as demonstrated by the above-cited excellent cycling stability of several high-voltage cathode materials. These results are even more impressive considering that the onset of the oxygen evolution reaction shifts by 59 mV per pH unit to more negative potentials when increasing the pH from ≤ 0 (e.g. sulfuric acid used in lead-acid batteries) to the usually near-neutral pH of water-in-salt electrolytes. In addition, lithium-ion insertion/intercalation potentials are shifted by $\geq 200 \text{ mV}$ to more positive potentials in water-in-salt electrolytes, further increasing the required oxidative stability.^{1,7}

For the cathodic scan, several studies suggest that the measured current density is the sum of several competing processes: hydrogen evolution reaction (HER), reduction of dissolved gases, and electrochemical anion reduction.^{1,3,7} There is growing evidence that the latter process leads to the formation of a solid electrolyte interphase (SEI) that consequently limits the HER.^{3,7} Recently, a different mechanism regarding the SEI formation process in water-in-salt electrolytes was proposed: According to this study, anion reduction is rather the result of nucleophilic attack by hydroxide anions that form as a byproduct of the HER.⁴ More work is needed to better understand the formation process and effectiveness of the SEI forming in water-in-salt electrolytes.

The measured current densities are also highly dependent on the catalytic activity of the electrode material, as illustrated in Fig. 2d. We observe significantly different current densities on platinum (1 mm disk electrode, eDAQ), gold, stainless steel, titanium (12 mm disk, $>99.6\%$, Goodfellow), glassy carbon (1 mm disk electrode, eDAQ), and aluminum (12 mm disk, $>99.3\%$, MTI). The differences in cathodic stability towards water reduction follow the reported trends for the catalytic activity of these materials.²⁷ For the anodic scan, the current density decreases in the order stainless steel \approx gold $>$ platinum $>$ glassy carbon $>$ titanium. Comparable differences in current density between different working electrode materials were also reported in literature.^{7,28}

Finally, quantification of electrolyte oxidation and reduction products resulting from the competition of different processes on the anode (hydrogen evolution, reduction of dissolved gases, anion reduction) and cathode side (oxygen evolution, current collector corrosion, and potentially anion oxidation) provide valuable additional insights, especially if conducted using composite battery electrodes as working electrodes. In particular, gas evolution studies are needed to demonstrate the real practicality of batteries based on water-in-salt electrolytes. A first such study was published recently.³

Summary

The water-in-salt approach has enabled aqueous batteries and supercapacitors with significantly larger cell voltages. However, as shown above, the ESW can easily differ by 1–1.5 V depending on the cut-off current density that is chosen for evaluating the voltammetry data. This sensitivity to the cut-off criterion has contributed to the disconnect between reported ESWs and reported cycling stability/Coulombic efficiency of batteries and supercapacitors incorporating water-in-salt electrolytes. In addition, the ESW of water-in-salt electrolytes strongly depends on the electrode material, as the high stability is a result of kinetic stabilizations that depend on the electrocatalytic properties of the electrode material. To give a more application-relevant assessment of the ESW of water-in-salt electrolytes, more stringent criteria should be used when extracting ESWs from voltammetry data. Ideally, the electrodes chosen for the ESW experiments would have similar electrocatalytic properties as the electrodes of the target device. In addition, all relevant experimental details such as cell type, electrode material, mass loading (if applicable), scan rate, and cut-off current density/data analysis method should be provided to allow assessment and comparison of ESW data from voltammetry.

Finally, more realistic cell tests using small amounts of electrolyte, high mass loadings, and low current rates are highly desirable. Such cells should also be subjected to constant voltage at various states-of-charge and to different temperatures to study their stability under various real-life conditions.

ORCID

Ruben-Simon Kühnel <https://orcid.org/0000-0003-1542-2970>

References

1. L. Suo, O. Borodin, T. Gao, M. Olguin, J. Ho, X. Fan, C. Luo, C. Wang, and K. Xu, *Science*, **350**, 938 (2015).
2. J. Vatamanu and O. Borodin, *J. Phys. Chem. Lett.*, **8**, 4362 (2017).

3. L. Suo et al., *J. Am. Chem. Soc.*, **139**, 18670 (2017).
4. N. Dubouis, P. Lemaire, B. Mirvaux, E. Salager, M. Deschamps, and A. Grimaud, *Energy Environ. Sci.*, **11**, 3491 (2018).
5. L. Suo, Y.-S. Hu, H. Li, M. Armand, and L. Chen, *Nat. Commun.*, **4**, 1481 (2013).
6. L. Suo et al., *Angew. Chem. Int. Ed.*, **55**, 7136 (2016).
7. Y. Yamada, K. Usui, K. Sodeyama, S. Ko, Y. Tateyama, and A. Yamada, *Nat. Energy*, **1**, 16129 (2016).
8. C. Yang et al., *Joule*, **1**, 122 (2017).
9. D. Reber, R.-S. Kühnel, and C. Battaglia, *ACS Mater. Lett.*, **1**, 44 (2019).
10. F. Wang, L. Suo, Y. Liang, C. Yang, F. Han, T. Gao, W. Sun, and C. Wang, *Adv. Energy Mater.*, **7**, 1600922 (2017).
11. F. Wang, Y. Lin, L. Suo, X. Fan, T. Gao, C. Yang, F. Han, Y. Qi, K. Xu, and C. Wang, *Energy Environ. Sci.*, **9**, 3666 (2016).
12. S. Ko, Y. Yamada, K. Miyazaki, T. Shimada, E. Watanabe, Y. Tateyama, T. Kamiya, T. Honda, J. Akikusa, and A. Yamada, *Electrochem. Commun.*, **104**, 106488 (2019).
13. H. Tomiyasu, H. Shikata, K. Takao, N. Asanuma, S. Taruta, and Y.-Y. Park, *Sci. Rep.*, **7**, 45048 (2017).
14. T. Liu, L. Tang, H. Luo, S. Cheng, and M. Liu, *Chem. Commun.*, **55**, 12817 (2019).
15. M. Becker, R.-S. Kühnel, and C. Battaglia, *Chem. Commun.*, **55**, 12032 (2019).
16. A. I. Mohamed and J. F. Whitacre, *Electrochim. Acta*, **235**, 730 (2017).
17. O. Borodin et al., *ACS Nano*, **11**, 10462 (2017).
18. K. Xu, *Chem. Rev.*, **104**, 4303 (2004).
19. P. Meister, H. Jia, J. Li, R. Kloepsch, M. Winter, and T. Placke, *Chem. Mater.*, **28**, 7203 (2016).
20. H. E. Darling, *J. Chem. Eng. Data*, **9**, 421 (1964).
21. J. Liu et al., *Nat. Energy*, **4**, 180 (2019).
22. K. Fröhlich, G. Bimashofer, G. Fafilek, F. Pichler, M. Cifrain, and A. Trifonova, *ECS Trans.*, **73**, 83 (2016).
23. J. Wojciechowski, Ł. Kolanowski, A. Bund, and G. Lota, *J. Power Sources*, **368**, 18 (2017).
24. Z. Lin, T. Liu, X. Ai, and C. Liang, *Nat. Commun.*, **9**, 5262 (2018).
25. J. Betz, G. Bieker, P. Meister, T. Placke, M. Winter, and R. Schmuch, *Adv. Energy Mater.*, **9**, 1803170 (2019).
26. M. P. S. Mousavi, A. J. Dittmer, B. E. Wilson, J. Hu, A. Stein, and P. Bühlmann, *J. Electrochem. Soc.*, **162**, A2250 (2015).
27. I. Roger, M. A. Shipman, and M. D. Symes, *Nat. Rev. Chem.*, **1**, 0003 (2017).
28. L. Coustan, G. Shul, and D. Bélanger, *Electrochem. Commun.*, **77**, 89 (2017).